MOLECULAR IMAGING AND BIOLOGY

Published Online: 8 September 2010

Mol Imaging Biol (2011) 13:985–994
DOI: 10.1007/s11307-010-0410-1

RESEARCH ARTICLE

Assessing p-Glycoprotein (Pgp) Activity *In Vivo* Utilizing ^{68}Ga–Schiff Base Complexes

Marco Fellner,[1] Wolfgang Dillenburg,[2] Hans-Georg Buchholz,[3] Nicole Bausbacher,[3] Mathias Schreckenberger,[3] Franz Renz,[4] Frank Rösch,[1] Oliver Thews[2]

[1]*Institute of Nuclear Chemistry, University of Mainz, Fritz Strassmann-Weg 2, 55128, Mainz, Germany*
[2]*Institute of Physiology and Pathophysiology, University Medicine Mainz, 55128, Mainz, Germany*
[3]*Department of Nuclear Medicine, University Hospital, 55101, Mainz, Germany*
[4]*Institute of Inorganic Chemistry, University of Hannover, 30167, Hannover, Germany*

Abstract

Purpose: The p-glycoprotein (Pgp) is the most prominent member of active drug transporters leading to a multidrug-resistant phenotype. For identification of tumors functionally over-expressing Pgp *in vivo*, non-invasive imaging techniques are needed.

Procedures: Six Schiff base compounds were synthesized and labeled with ^{68}Ge/^{68}Ga generator-derived ^{68}Ga. The compounds were studied *in vitro* in Pgp-positive tumor cells. The property of being a Pgp substrate was tested by comparison of the tracers uptake in R-3327 Dunning prostate carcinoma AT1 cells in presence and absence of the Pgp-inhibitor verapamil. *In vivo* investigations were performed with tumor-bearing rats imaged with micro-positron emission tomography.

Results: All ligands were labeled with ^{68}Ga in yields of >92% beside one (~55%). The tracers showed different accumulation within the cells *in vitro* (4–60%). In blocking experiments, the ratio (blocked to unblocked) varied from 1.8 to 1.0. For *in vivo* experiments, ^{68}Ga–ENBDMPI and ^{68}Ga–MFL6.MZ were selected. The tumors showed specific uptake of the tracer. Direct intratumoral injection of verapamil increased the tracer concentration by ~25% reflecting the functional Pgp activity.

Conclusions: Two ^{68}Ga-labeled ligands appear to be valuable for imaging non-invasively the intratumoral Pgp activity. On a long term, patients with multidrug-resistant tumors pre-therapeutically may be identified prior to treatment.

Key Words: Functional activity, P-glycoprotein, PET tracer, Tumors, ^{68}Ga

Abbreviations: Pgp, p-glycoprotein; VPL, verapamil; MDR, multidrug resistance

Introduction

The p-glycoprotein (Pgp) is a 170-kDa protein located in the cell membrane which transports a broad spectrum of drugs (with size from less than 200 Da to almost 1,900 Da and amphiphilic structure) out of the cell [1]. This protein is the most prominent and best studied member of the ATP-binding cassette family, which can be found in numerous tissues such as kidney, liver, brain, or placenta [1, 2]. Since many tumors overexpress Pgp and several anti-tumoral drugs are substrates, this transporter is responsible for the phenomenon of multidrug resistance (MDR) in human tumors, thereby limiting the cytotoxic efficacy of chemotherapy [2, 3]. Since more or less specific inhibitors of the transport protein are known, one strategy to overcome MDR is the reduction of the functional transport capacity. However, even though some promising agents have been identified and underwent clinical testing, at present the search of an ideal non-toxic drug sufficiently inhibiting Pgp transport has not been accomplished [4]. In addition, MDR does not play a role in all tumor patients. Only patients

Correspondence to: Frank Rösch; *e-mail:* frank.roesch@uni-mainz.de

(over)expressing Pgp might benefit from a simultaneous inhibitor treatment. For this reason, these patients should be identified in the clinical setting previously to chemotherapy in order to adapt the treatment regime to the individual demands, eventually changing to another treatment modality such as radiotherapy or surgery.

From this background, diagnostic methods are needed to assess the patient's individual tumor cells Pgp activity. With PET, this challenge would be approached non-invasively resulting not only in a value of the mean Pgp transport activity but also to quantify regional differences within the tumor tissue. PET-based imaging of chemoresistance would also help in the development of new, more specific Pgp inhibitors.

Several approaches have been published to visualize the activity or expression of Pgp in order to quantify the MDR of tumors or normal tissues. Most attempts used ^{99m}Tc-Sestasmibi (a tracer approved for cardiac imaging, which is known to also be a substrate of the Pgp) using the single photon emission computed tomography (SPECT) technique [5, 6]. However, due to the higher spatial and faster kinetic resolution of quantitative positron emission tomography (PET), few tracers were labeled with positron emitters to visualize MDR. Most of these approaches used carbon-11 labeled drugs known to be Pgp substrates (e.g., paclitaxel) [7, 8]. Several studies were performed using ^{11}C-verapamil (for an overview see [8]). However, verapamil is a Pgp substrate with a very high affinity to the transporter [9] which is the reason of this drug being a functional Pgp-inhibitor. Thus, ^{11}C-verapamil does not reflect the dynamic transport activity of the drug transporter.

While ^{11}C-carbon is cyclotron-produced, non-cyclotron dependent PET tracers, i.e., radionuclide generator-based derivatives, would provide another route to Pgp-tracer synthesis. The germanium-68/gallium-68 system ($T_{1/2}$(^{68}Ge)= 270.8 days), generating the positron emitter ^{68}Ga ($T_{1/2}$= 67.7 min; 89% positron branching), represents a promising example. Using the recently published generator post-processing, it is an excellent source for synthesizing and evaluating new tracers [10, 11].

Very few studies have been performed in which $^{67/68}$Ga-compounds were used to visualize the functional Pgp activity [12, 13]. In the case where the tracer itself is a substrate of Pgp, the intratumoral concentration would inversely reflect the Pgp transport activity. While the compound passively diffuses into the tumor cell, it has to be carried out actively by Pgp. This transport, therefore, should be inhibitable by known Pgp inhibitors.

The aim of the present study was the development of various new ^{68}Ga-labeled PET tracers for imaging the functional transport activity of Pgp. The use of ^{68}Ga as positron emitter would allow a convenient and fast synthesis at the site of PET scanning. The molecular structure of the ^{68}Ga-labeled tracer, however, has to be optimized to lead to a maximal enrichment in the tumor, combined with significant specificity as well as the inhibitability of the tracer efflux *via* Pgp.

Materials and Methods

Chemicals

All chemicals were used as supplied without further purification. 2,2-Dimethyl-1,3,propanediamine and potassium iodide were obtained from Merck. Dibromoethane and dry solvents were purchased from Fluka; ethanol (+2% MEK), potassium hydroxide, and 5-bromo-3-methoxysalicylaldehyde were obtained from Acros Organics. All other organic reagents were purchased from Sigma-Aldrich. Thin-layer chromatography was carried out on Merck SG 60 F254 and RP-18 F254s plates. ^{68}Ga generators were obtained from Cyclotron Co Ltd, Obninsk, Russian Federation. Starting activities ranged from 65 to 280 MBq.

Ligand Synthesis

(1) Bis(N,N'-amino-2,2-dimethylpropan)ethylenediamine (Fig. 1): Synthesis of the tetraamine was carried out as followed. To a cooled solution of 2,2-dimethyl-1,3-propanediamine (60.7 g, 0.63 mol) in 95% ethanol, 1,2-dibromoethane (24.0 g, 0.13 mol) was added drop wise over 2 h. The reaction was heated to reflux for 2 h and stirred for additional 12 h at 50°C. After cooling potassium hydroxide (25.0 g) was added and again heated to reflux for 30 min. The precipitate from the cooled solution was filtered and washed with cold ethanol. The solution was evaporated to oil and excess of the diamine was distilled at reduced pressure (6–8 mbar, 45°C). The residue was dissolved in diethyl ether, filtrated, and evaporated. Product was distilled at reduced pressure, giving a clear liquid (0.1 mbar, 110°C) yield: 10.5 g (35%), ^{1}H NMR (300 MHz, $CDCl_3$) δ (ppm)=0.83 (s, 12H), 1.32 (bs, 6H), 2.37 (bs, 4H), 2.49 (s, 4H), 2.65 (s, 4H)

General synthesis of ligands (2–7) (Fig. 2): 1.65 mmol of the corresponding salicylaldehyde was dissolved in 10–15 mL dry dichloromethane together with molecular sieve 4A. Compound (1) (125 mg, 0.54 mmol) in 1 mL dichloromethane was added, and the mixture was shaken overnight at room temperature. The molecular sieve was filtered off, washed with 5 mL dichloromethane, and the resulting solution was evaporated under reduced pressure leading to yellow to orange solids. Products were dried for 2 days under high vacuum. No further purification was needed.

(2) MFL1.MZ (2-(2-hydroxyphenyl)-1,3-bis[4-aza-5-(2-hydroxyphenyl)2,2-dimethyl-but-4-ene-1-yl]-1,3-imidazolidine): yield—98%, ^{1}H NMR (300 MHz, $CDCl_3$) δ (ppm)=0.79 (s, 6H), 0.81 (s, 6H), 2.25 (d, 2H), 2.53 (d, 2H), 2.64 (d, 2H), 3.02 (d, 2H), 3.39 (d, 2H), 3.54 (d, 2H), 3.72 (s, 1H), 6.91 (m, 3H), 6.83 (m, 3H), 7.23 (m, 6H), 8.07 (s, 2H), 10.09 (s, 1H), 13.58 (s, 2H)

(3) ENBDMPI (2-(2-hydroxy-3-ethoxyphenyl)-1,3-bis[4-aza-5-(2-hydroxy-3-ethoxyphenyl)-2,2-dimethyl-but-4-ene-1-yl]-1,3-imidazolidine): yield—97%, ^{1}H NMR (300 MHz, $CDCl_3$) δ (ppm)= 0.78 (s, 6H), 0.80 (s, 6H), 1.37 (t, 3H), 1.46 (t, 6H), 2.27 (d, 2H), 2.52 (d, 2H), 2.64 (q, 2H), 3.02 (d, 2H), 3.37 (d, 2H), 3.50 (q, 2H), 3.75 (s, 1H), 4.02 (q, 2H), 4.08 (q, 4H), 6.70 (m, 7H), 6.86 (d, 2H), 8.03 (s, 2H), 10.25 (s, 1H), 14.08 (s, 2H)

(4) MFL3.MZ (2-(2-hydroxy-3,5-ditertbutylphenyl)-1,3-bis[4-aza-5-(2-hydroxy-3,5-ditertbutylphenyl)-2,2-dimethyl-but-4-ene-1-yl]-1,3-imidazolidine): yield—98%, ^{1}H NMR (300 MHz, $CDCl_3$) δ (ppm)=0.77 (s, 6H), 0.79 (s, 6H), 1.27 (m, 27H), 1.39 (m, 27H), 2.30 (d, 2H), 2.54 (d, 2H), 2.65 (q, 2H), 2.93 (d, 2H), 3.42 (d, 2H),

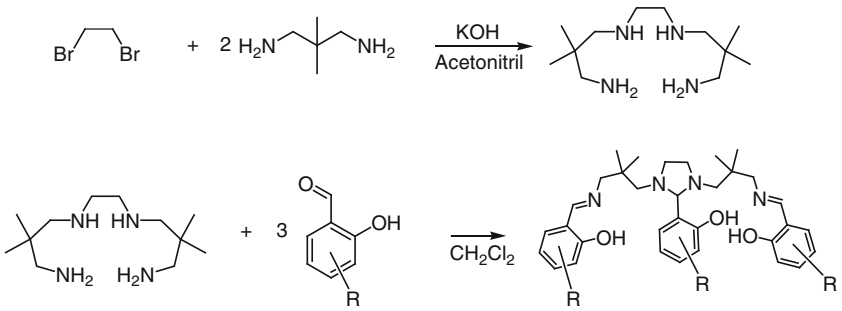

Fig. 1. General synthesis scheme of ligands.

3.56 (q, 2H), 3.75 (s, 1H), 6.79 (d, 1H), 7.02 (d, 2H), 7.20 (d, 1H), 7.34 (d, 2H), 8.18 (s, 2H), 10.54 (s, 1H), 13.79 (s, 2H)

(5) MFL4.MZ (2-(2-hydroxy-5-tertbutylphenyl)-1,3-bis[4-aza-5-(2-hydroxy-3,5-ditertbutylphenyl)-2,2-dimethyl-but-4-ene-1-yl]-1,3-imidazolidine): yield—98%, ^{1}H NMR (300 MHz, $CDCl_3$) δ (ppm)=0.77 (s, 6H), 0.79 (s, 6H), 1.27 (m, 27H), 2.27 (d, 2H), 2.54 (d, 2H), 2.65 (d, 2H), 3.02 (d, 2H), 3.40 (d, 2H), 3.53 (q, 2H), 3.72 (s, 1H), 3.91 (s, 2H), 6.66 (d, 1H), 6.83 (d, 1H), 7.07 (d, 1H), 7.17 (m, 2H), 7.31 (m, 3H), 8.17 (s, 2H), 10.04 (s, 1H), 13.34 (s, 2H)

(6) MFL5.MZ (2-(2-hydroxy-3-methoxy-5-bromophenyl)-1,3-bis[4-aza-5-(2-hydroxy-3-methoxy-5-bromophenyl)-2,2-dimethyl-but-4-ene-1-yl]-1,3-imidazolidine): yield—98%, ^{1}H NMR (300 MHz, $CDCl_3$) δ (ppm)=0.78 (s, 6H), 0.80 (s, 6H), 2.23 (d, 2H), 2.50 (d, 2H), 2.63 (q, 2H), 3.10 (d, 2H), 3.36 (d, 2H), 3.49 (d, 2H), 3.67 (s, 1H), 3.77 (s, 3H), 3.86 (s, 6H), 6.69 (d, 1H), 6.74 (d, 1H), 6.88 (d, 2H), 6.92 (d, 2H), 7.96 (s, 2H), 10.28 (s, 1H), 14.24 (s, 2H)

(7) MFL6.MZ (2-(2-hydroxy-5-bromophenyl)-1,3-bis[4-aza-5-(2-hydroxy-5-bromophenyl)-2,2-dimethyl-but-4-ene-1-yl]-1,3-imidazolidine): yield—98%, ^{1}H NMR (300 MHz, $CDCl_3$) δ (ppm)=0.80 (s, 6H), 0.82 (s, 6H), 2.23 (d, 2H), 2.50 (d, 2H), 2.63 (q, 2H), 3.08 (d, 2H), 3.36 (d, 2H), 3.53 (q, 2H), 3.66 (s, 1H), 6.59 (d, 1H), 6.80 (d, 2H), 7.03 (d, 1H), 7.15 (d, 1H), 7.27 (d, 2H), 7.32 (d, 1H), 7.35 (d, 1H), 8.01 (s, 2H), 9.82 (s, 1H), 13.48 (s, 2H)

Reference Ga-Complex Formation

(8) Ga–MFL6.MZ: Compound (7) (115 mg, 0.5 mmol) was dissolved in 10 mL methanol, and $Ga(acac)_3$ (183 mg, 0.5 mmol) in 2 mL methanol was added. The solution was heated to reflux for 30 min. To the cooled solution, KI (100 mg, 0.6 mmol) in water was added. Slow evaporation of the solvent over 4 weeks yielded yellow crystals suitable for X-ray analysis.

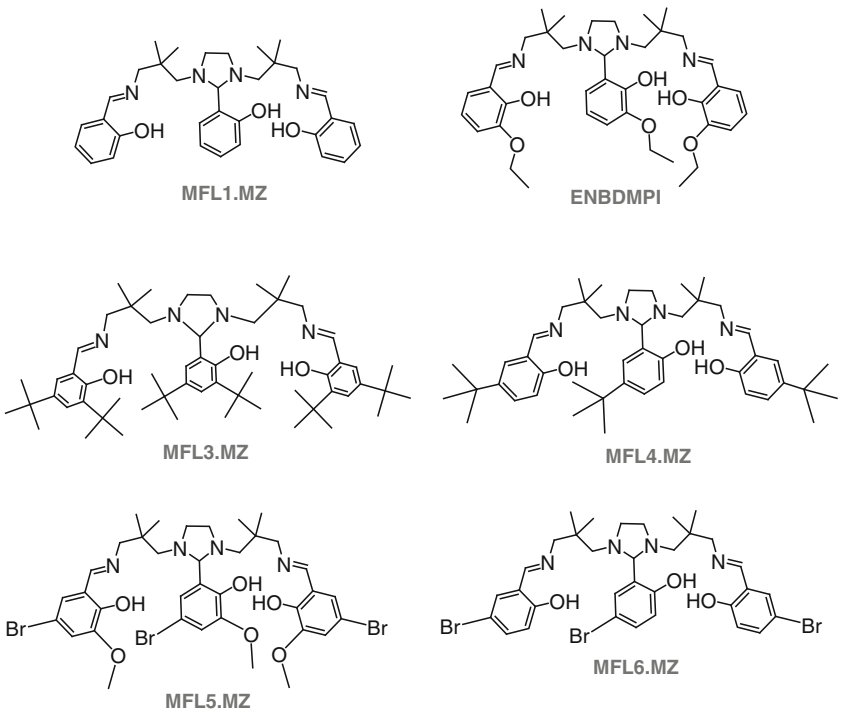

Fig. 2. Ligands investigated in this study (MFL1.MZ–MFL6.MZ and ENBDMPI).

^{68}Ga-radiolabeling

^{68}Ga-labeling: Elution of the ^{68}Ge/^{68}Ga generator and purification of the eluate was carried out as described [10, 11]. In brief, ^{68}Ga is eluted from the generator with 10 mL 0.1 M HCl and is online immobilized on an acidic cation exchanger. Metal impurities are removed by 1 mL of a mixture of acetone and hydrochloric acid (80% acetone/0.15 M HCl). Subsequently, ^{68}Ga is eluted quantitatively in 400 µL of a second mixture of acetone and HCl (97.6% acetone/0.05 M HCl) from the cation exchanger. This fraction serves as an ideal low volume, low acidic, and chemically highly pure source of ^{68}Ga for subsequent labeling.

Labeling was performed with 20–40 µL of a ligand solution (1 mg/mL in ethanol, 30 nmol for each ligand) in 400 µL 0.12 M HEPES sodium salt buffer at pH=4.3 by addition of the purified ^{68}Ga-fraction in 1.5 mL Eppendorf vials at different temperatures (room temperature to 80°C) within 1–10 min (Fig. 3). Determination of radiochemical labeling yield and complex formation kinetics were carried out by TLC on silica and RP-18 plates with 90% methanol/10% isotonic saline and were measured on a Canberra Packard Instant Imager.

Purification of low yielding complexes was carried out by passing the reaction mixture over a Sep-Pak silica cartridge with subsequent elution by 1 mL ethanol. For labeling yields >92%, no further purification was carried out; only the pH was adjusted to ~7 by addition of 8.7 µL 1 M sodium hydroxide. This solution was applicable for *in vitro* and *in vivo* measurements with a total volume of 0.5 mL.

Determination of the Partition Coefficient (Log D)

The partition coefficient at pH 7.4 and therefore the lipophilicity was measured as follows. Each ^{68}Ga-complex was immobilized on a Waters C18 light cartridge or a Merck Silica cartridge (for ^{68}Ga–MFL3.MZ), respectively, from the reaction mixture, washed with 1 mL water, and eluted with 2 mL ethanol. The ethanol was evaporated and the tracer resuspended in phosphate-buffered saline (PBS) buffer. Of this solution, 700 µL was added to 700 µL octanol and mixed for 2 min at 1,500 min^{-1} at room temperature in a HLC Biotech HeatingThermoMixer MHR 13. After centrifugation at 12,000 min^{-1} for 2 min, a 3 µL aliquot of the octanol and the water layer was spotted on paper and counts were measured in a Canberra Instant Imager. Of the octanol layer, 400 µL was removed and added to 300 µL octanol and 700 µL PBS buffer. The procedure was repeated, and the partition coefficient was calculated as the ratio of CPM of octanol to CPM of water. Experiments were conducted in quadruplicate, and the average log D value of two back extractions for the four trials was reported.

Tumor and Animal Model

The subline AT1 of the rat R-3327 Dunning prostate carcinoma was used in all experiments. This cell line functionally expresses Pgp [14]. Cells were grown in RPMI medium supplemented with 10% fetal calf serum (FCS) at 37°C under a humidified 5% CO_2 atmosphere and sub cultivated once per week. Prior to the experiments, cells were transferred to RPMI medium without additional FCS supplementation for 24 h.

For *in vivo* experiments male Copenhagen rats (Charles River Wiga, Sulzfeld, Germany; body weight 150 to 200 g) housed in the animal care facility of the University of Mainz were used in this study. Animals were allowed access to food and acidified water *ad libitum* before the investigation. All experiments had previously been approved by the regional animal ethics committee and were conducted in accordance with the German Law for Animal Protection and the UKCCCR Guidelines [15]. Solid carcinomas of the R3327-AT1 cell line were heterotopically induced by injection of AT1 cells (approximately 0.4 mL 10^4 cells/µL) subcutaneously into the dorsum of the hind foot. Tumors grew as flat, spherical segments and replaced the subcutis and corium completely. Volumes were determined by measuring the three orthogonal diameters (d) of the tumors and using an ellipsoid approximation with the formula: $V = d_1 \times d_2 \times d_3 \times \pi/6$. Tumors were used when they reached a volume of between 1.0 and 2.0 mL approximately 10 to 14 days after tumor cell inoculation.

Tracer Uptake Assay In Vitro

In order to assess the functional activity of Pgp, the uptake of the proposed ^{68}Ga tracer into tumor cells in the presence or absence of a specific Pgp-inhibitor (verapamil) was determined. This technique (using fluorescent Pgp substrates) has been shown to be a suitable parameter of the Pgp activity [16]. After keeping the cells in serum-free medium for 24 h prior to the experiments, the cells were incubated with the tracer in medium (only pmol of the ^{68}Ga-tracer together with the uncomplexed ligand, together 30 nmol). In a second set of experiments, cells were incubated with a combination of the tracer and verapamil (VPL) at a concentration of 10 µM (stock solution 5 mM, dissolved in ethanol). After incubation at 37°C for 30 min, the cells were centrifuged and the activity of the supernatant as well as of the cell pellet was determined separately in a curiemeter (M2316, Messelektronik Dresden GmbH, Germany). The tracer is taken up into the cell by passive diffusion. The fraction

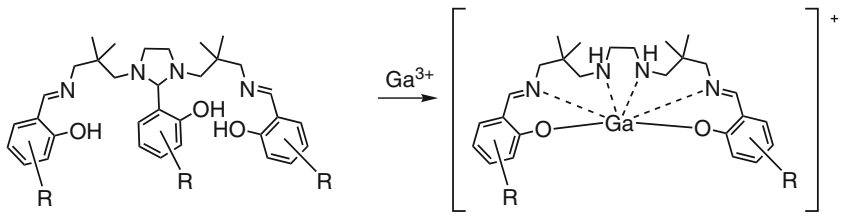

Fig. 3. Complex formation of ligands with Ga^{3+} by ring opening and subsequent formation of the octahedral monocationic complex.

of the activity kept in the cell pellet is therefore a measure for the cellular uptake into the cell and is mainly affected by the lipophilic solubility of the tracer. Since VPL inhibits the active efflux of Pgp substrates, the intracellular concentration will be higher in the presence of verapamil. The activity ratio in the presence and absence of VPL can therefore be used as a measure of Pgp activity.

Animal PET Studies

For PET imaging, the tracers, ^{68}Ga–ENBDMPI and ^{68}Ga–MFL6.MZ, were used. Rats were anesthetized with pentobarbital (40 mg/kg, i.p., Narcoren, Merial, Hallbergmoos, Germany), and a catheter was inserted into the left jugular vein for radiotracer application and a tube was placed in the trachea. The PET imaging was performed on a microPET Focus 120 small animal PET (Siemens/Concorde, Knoxville, USA). During PET measurements, the animals were placed in supine position and breathed room air spontaneously through a tracheal tube. Dynamic PET studies were acquired in 3D mode for 60 min with a mean activity of 40.3±3.8 MBq (^{68}Ga–MFL6.MZ) and 36.7±3.6 MBq (^{68}Ga–ENBDMPI). The radiotracer was administered as a bolus injection via the catheter in the left jugular vein of each animal. The PET list mode data was histogrammed into 14 frames and reconstructed using OSEM algorithm. Volumes of interests were defined for tumor and reference tissue (testis). Ratios of tumor to reference tissue were calculated from integral image between 30' and 60' after tracer injection.

In order to assess whether tracer accumulation is correlated with the Pgp activity in the tissue, Pgp was inhibited *in vivo* by intratumoral injection of VPL. Therefore, verapamil was dissolved in ethanol at a concentration of 1 mM. Small amounts of this solution (10 µL/mL tumor volume) were injected directly into one of the tumors of the animals 10 min prior to tracer injection leading to a tissue concentration comparable of that used in the cell experiments. The contralateral tumor of each animal served as a control. In this tumor the same amount of ethanol alone, i.e., without the ^{68}Ga-compounds was injected.

Biodistribution Measurements

In order to assess the distribution of the tracer ^{68}Ga–MFL6.MZ in different organs of the animals, the tracer was injected i.v. in anesthetized tumor-bearing rats. After 60 min, the animals were euthanized, and different organ (blood, brain, heart, kidney, liver, lung, spleen, testis) and tumor samples were taken. The tissue samples were weighed and dissolved in 5 mL 4 M KOH at 75°C for 30 min. Finally, the ^{68}Ga activity in the organs was measured in a gamma counter (Perkin Elmer 2470 Wizard^2).

Statistical Analysis

Results are expressed as means±SEM. Differences between groups were assessed by the two-tailed Wilcoxon test for paired or unpaired samples. The significance level was set at α=5% for all comparisons.

Results

Chemistry

Synthesis of the ligands resulted in products of high yields (>97%) and high purity. Complexation of MFL6.MZ with $Ga(acac)_3$ affords crystals suitable for X-ray structure

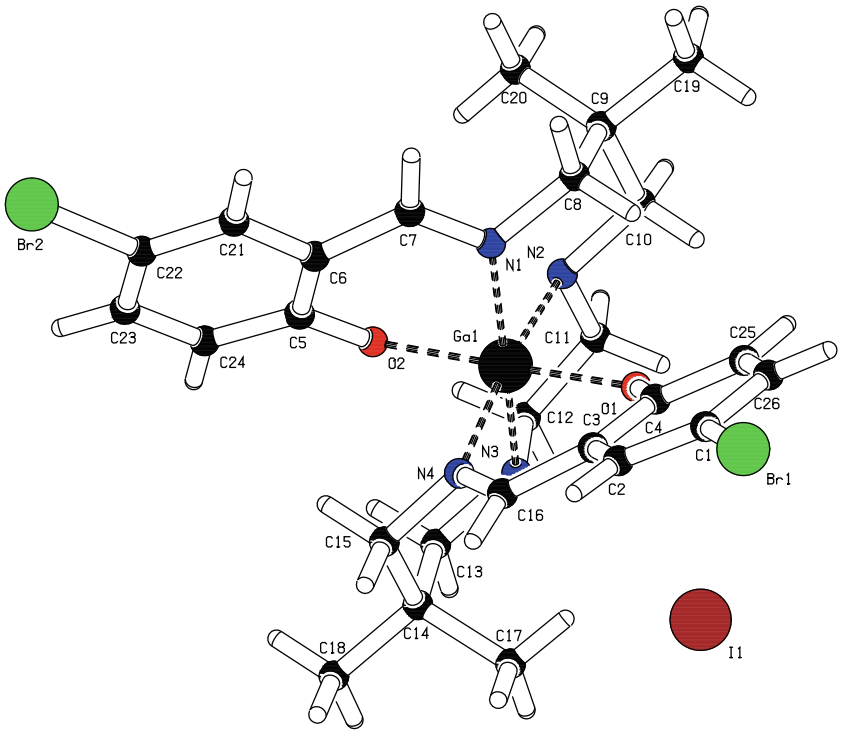

Fig. 4. X-ray structure of inactive $[Ga(MFL6.MZ)]^+I^-$ complex.

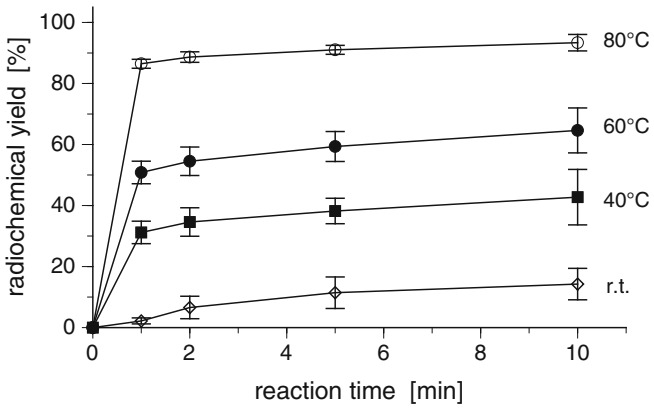

Fig. 5. ^{68}Ga-labeling kinetics of MFL6.MZ (30 nmol ligand, 400 µL 0.12 M Na–HEPES buffer, r.t. to 80°C, 1–10 min). Values are expressed as means±SD of three experiments.

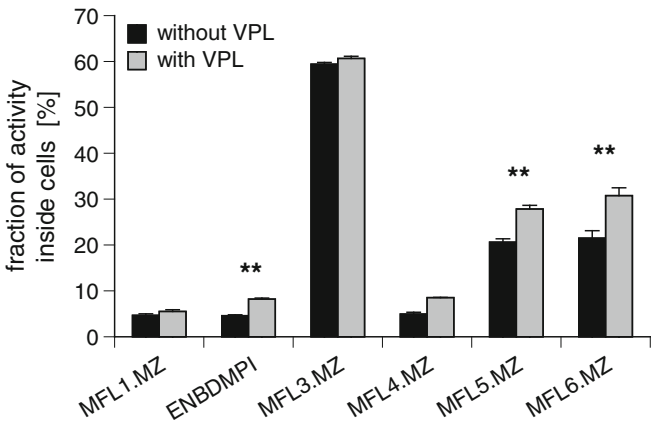

Fig. 6. Fraction of ^{68}Ga activity within AT1 cells after 30 min of incubation with various tracers in the presence and absence of verapamil (VPL). Values are expressed as means±SEM of three to nine experiments; $^{**}p<0.01$ with VPL *vs.* without VPL.

determination (Fig. 4). This revealed the estimated octahedral monocationic complex with four nitrogen and two phenolic oxygen donors.

Labeling with generator-derived ^{68}Ga in HEPES buffer by addition of the purified ^{68}Ga fraction is fast and efficient. Fig. 5 shows kinetics of ^{68}Ga–MFL6.MZ complex formation. The labeling yields of the investigated ligands after 10 min heating at 75°C were >92% for all compounds beside MFL3.MZ which showed only ~55%. However, ^{68}Ga–MFL3.MZ could be purified in a second step in a fast and easy method using commercially available silica solid phase separation cartridges leading to radiochemical purity of >95%. For all the other ^{68}Ga–Schiff base complexes with labeling yields >92%, further purification was not performed.

Determining the partition coefficients of the compounds showed that the average log D value of two back extractions varied between 1.60 and 3.20 (Table 1) and is only dependent on the aromatic substituents of the ligand structure. It is a helpful indicator for the passive uptake of compounds into the cell. However, it is not a prejudification for determination of transport ability of the ^{68}Ga-tracer by Pgp.

In Vitro and In Vivo Studies

An applicable tracer for measuring the Pgp activity has to fulfill two features: (1) it should enter the cell easily (by passive diffusion) and (2) the tracer should be a substrate of the Pgp and this transport should be inhibitable by Pgp inhibitors (e.g., verapamil). In order to measure the passive uptake of the ^{68}Ga–Schiff base complexes, cells were incubated with the tracer for 30 min after which the suspension was centrifuged and the activity in the cells as well as in the supernatant was determined. In a second series, the cells were incubated in the presence of VPL. Fig. 6 shows the fraction of ^{68}Ga-complexes detected inside the cells for all tracers in the absence or presence of VPL. The ligand ENBDMPI was described by Sharma *et al.* [12]. Since the cytocrit of the cell suspension was only 0.28±0.05%, all tracers show a specific enrichment in the cells. However, the passive uptake was much more pronounced with the ^{68}Ga–MFL6.MZ tracer. In this case, more than 20% of the tracer was found within the cells. The tracer ^{68}Ga–MFL3.MZ, which was most lipophilic (Table 1), shows the largest enrichment in the cellular compartment (Fig. 6), presumably in the cell membrane.

All tracers were identified to be substrate of the Pgp since the active efflux could be inhibited by verapamil resulting in a higher intracellular concentration (Fig. 6). In the presence of VPL the concentration of ^{68}Ga–ENBDMPI was 178±5% of that without VPL, whereas for ^{68}Ga–MFL6.MZ, the ratio was 144±3%. The efflux transport of the lipophilic tracer ^{68}Ga–MFL3.MZ which shows the highest cellular accumulation showed only a negligible dependency on VPL indicating the Pgp plays only a minor role for the transport of this substance.

From these *in vitro* experiments it became evident that ^{68}Ga-MFL6.MZ showed the best compromise of good passive uptake into the cells and pronounced Pgp-mediated efflux inhibitable by VPL. For this reason further *in vivo* experiments were performed with this tracer and (for comparison) with ^{68}Ga–ENBDMPI which is the compound described by Sharma *et al.* [12].

Table 1. Lipophilicity of the compounds expressed by the partition coefficient

Compound	Log D
^{68}Ga–MFL1.MZ	1.60±0.03
^{68}Ga–ENBDMPI	2.03±0.09
^{68}Ga–MFL3.MZ	3.20±0.15
^{68}Ga–MFL4.MZ	2.43±0.12
^{68}Ga–MFL5.MZ	2.72±0.14
^{68}Ga–MFL6.MZ	2.49±0.07

Values are expressed as means±SD (n=8)

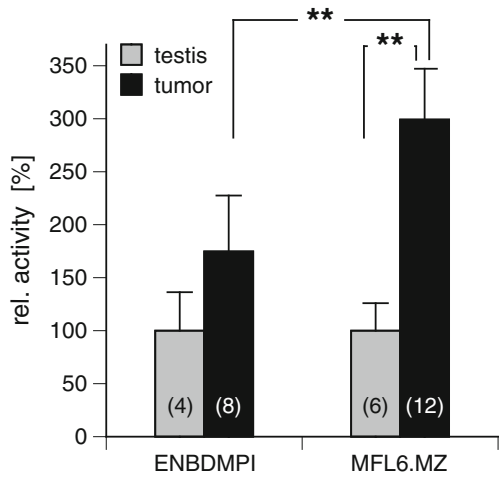

Fig. 7. Accumulation of ^{68}Ga–ENBDMPI and ^{68}Ga–MFL6.MZ in AT1 tumors and a reference tissue (testis) *in vivo*. Values are expressed as means±SEM; $^{**}p<0.01$; number of tumors in *brackets*.

Subsequently, both tracers were used in PET experiments with tumor-bearing rats. Fig. 7 shows the averaged activity in tumor and testes between 6 and 60 min of the measuring period. ^{68}Ga–MFL6.MZ is strongly accumulated in the tumor resulting in a three times higher concentration as compared to the reference tissue. ^{68}Ga–ENBDMPI is enriched to a much smaller extent in the tumor by only 74% (μ-PET image shown in Fig. 8). These results are in good accordance to the cell culture experiments (Fig. 6).

In order to assess whether the ^{68}Ga–MFL6.MZ concentration in the tumor is dependent on the Pgp activity, 10 to 20 μL of 1 mM verapamil solution was injected directly into one of the two tumors of an animal. The contralateral tumor served as control by injecting the same amount of ethanol. Fig. 9 shows an example of these experiments. The tumor with the VPL injection shows locally a higher tracer accumulation as the contralateral control tumor. These results correspond well to the cell culture experiments (Fig. 6). Fig. 10 shows the results of four animals. The data

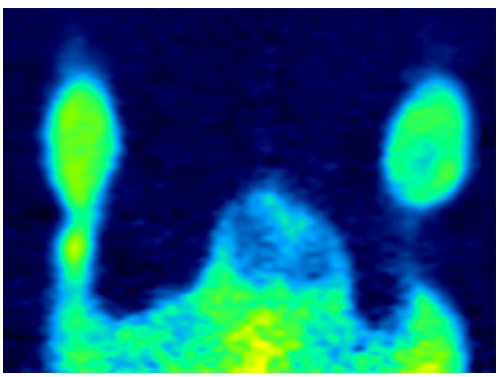

Fig. 8. μ-PET image of ^{68}Ga–ENBDMPI accumulation in AT1 tumors (summed 30' to 60' p.i.).

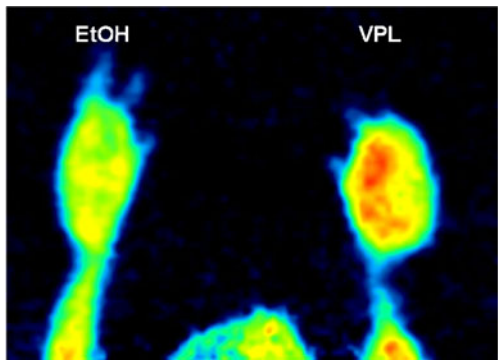

Fig. 9. Example of ^{68}Ga–MFL6.MZ accumulation in AT1 tumors between 30' and 60' p.i. In the *right tumor* ("VPL") 20 μL of verapamil solution (1 mM in EtOH) was injected. The contralateral tumor received the same volume of EtOH alone ("EtOH").

clearly demonstrate that VPL injection leads to a much higher tracer accumulation (factor 1.3) as a consequence of an inhibited Pgp activity resulting in a reduced ^{68}Ga–MFL6.MZ efflux out of the cells.

Table 2 finally shows the distribution of ^{68}Ga–MFL6.MZ in the blood and different organs. The highest concentrations were found in the liver and the kidney (40- and 103-times higher than in the blood). The concentrations in heart, spleen, and tumor were markedly lower. The lowest ^{68}Ga–MFL6.MZ level was found in the brain which is maybe the result of an active Pgp transport out of the brain tissue at the blood–brain barrier.

Discussion

Since the activity of the Pgp transporter is of high importance not only in oncology (multidrug resistance of tumors) but also in neurology/psychiatry (drug uptake through the blood–brain barrier), the measurement of this

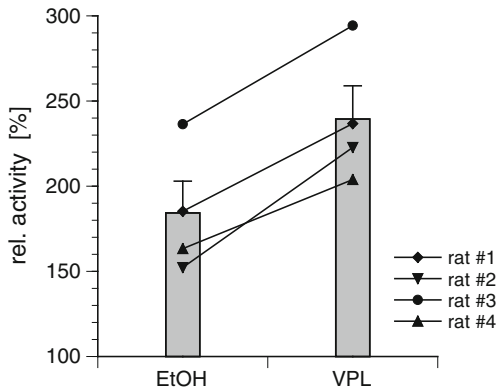

Fig. 10. Impact of verapamil injection into the tumor tissue *in vivo* on the accumulation of ^{68}Ga–MFL6.MZ between 30' and 60' p.i. expressed as the relative activity related to the testis. Verapamil was injected into one of the two implanted tumors ("*VPL*"). The contralateral tumor of the same animal served as control (injection of an equivalent volume of EtOH, "*EtOH*"). Values are expressed as means±SEM.

Table 2. Biodistribution of ^{68}Ga–MFL6.MZ in tumor-bearing rats 60 min after injection

Tissue	%ID/g tissue	Tissue-to-blood ratio
Blood	0.08±0.01	
Lung	0.45±0.03	5.9
Heart	0.89±0.02	12
Spleen	0.97±0.06	13
Liver	3.01±0.08	39
Kidney	7.94±0.19	103
Testis	0.05±0.01	0.4
Brain	0.03±0.01	0.7
Tumor	0.17±0.02	2.3

Values are expressed as means±SEM of the injected dose (2.6±0.1 MBq) normalized to 1 g of tissue (n=3 experiments)

parameter is of importance for the clinical setting. For this reason, imaging techniques have been developed to non-invasively assess the Pgp transport rate. Positron emitter-labeled substrates or blockers of the Pgp have used mostly carbon-11 labeled compounds to visualize the Pgp activity by means of PET (e.g., for determining the role of the Pgp and the blood–brain barrier [17, 18]). These experiments revealed the possibility of functional imaging with PET. However, ^{11}C is a radionuclide with a short half-life time (20 min) that has to be produced at a cyclotron, which makes this positron emitter less suitable for clinical routine. Radionuclides, which can be obtained directly in the laboratory (generator-based tracers), would be beneficial. Besides PET, SPECT has been used to assess the Pgp activity [5, 6, 19]. However, positron emitters for PET have a higher spatial resolution compared to SPECT and provide quantitative biochemical and physiological parameters.

Starting with the compound [^{68}Ga(3-ethoxy-ENBDMPI)]$^{+}$ described by Sharma and coworkers [12, 13], various ^{68}Ga-labeled Schiff base-based tracers differing in side chains and substituents have been synthesized. Labeling the desired ligands with ^{68}Ga in HEPES buffer is much faster than the procedure published by Sharma *et al.* As the intermediate synthesis of ^{68}Ga(acac)$_3$ is avoided, the reaction time is only 20 min starting from elution of the generator (compared to 60 min with the preparation of the ^{68}Ga-acetylacetonate synthon [12, 13]). The radiochemical yields are comparable to the procedure described by Sharma and coworkers, however with a shorter reaction time (~25 min compared to 60 min by Sharma), higher batch activities and specific activities can be achieved.

The ability of using these ^{68}Ga-compounds depends mainly on their cellular uptake and the Pgp-mediated efflux. The first parameter was evaluated *in vitro* by the accumulation of ^{68}Ga-complexes in the cellular compartment. With respect to this parameter, the various tracers differed profoundly. Taking into account that the volume fraction of the cells (cytocrit) was only ~0.3%, the concentration ratio between cells and medium was approximately 16:1 for the tracers ^{68}Ga–MFL1.MZ, ^{68}Ga–ENBDMPI, and ^{68}Ga–MFL4.MZ. For ^{68}Ga–MFL5.MZ and ^{68}Ga–MFL6.MZ, the cellular concentration was ~90 times higher than in the medium, whereas ^{68}Ga–MFL3.MZ showed a concentration ratio of 490. The extremely high uptake of ^{68}Ga–MFL3.MZ seems to be the result of a high lipophilicity (Table 1) leading to a very high passive permeation through the cell membrane. These results clearly demonstrate that all ^{68}Ga-labeled compounds show a marked uptake and accumulation in tumor cells. High cellular tracer concentrations are important for a good signal-to-noise ratio of the PET signal. From this point of view, the ligand MFL3.MZ appears to be most suitable, but also MFL5.MZ and MFL6.MZ are promising.

As a second aspect for a suitable Pgp tracer is that the compound is a substrate for Pgp, the compounds efflux in a Pgp-expressing cell should be inhibitable by Pgp-inhibitor (e.g., verapamil), leading to an increased intracellular concentration of the ^{68}Ga-complex. For this reason the ratio of cellular concentration of a Pgp substrate in the presence and absence of verapamil could be used as an indicator of the Pgp-mediated transport rate of the tracer [16]. This ratio was ~1.2 for ^{68}Ga–MFL1.MZ, ~1.7 for ^{68}Ga–ENBDMPI and ^{68}Ga–MFL4.MZ, and ~1.4 for ^{68}Ga–MFL5.MZ and ^{68}Ga–MFL6.MZ. Only for the lipophylic tracer ^{68}Ga–MFL3.MZ (which showed the most pronounced cellular accumulation), inhibition of Pgp had practically no impact on the cellular tracer accumulation (Fig. 6). This relatively small effect of Pgp inhibition seems to be the result of non-specific binding to membranes and lipophilic compartments of the cells.

In the present study, the concentration ratio between blocked and unblocked cells for the compound ^{68}Ga–ENBDMPI was only 1.78 and thus smaller than in the experiments by Sharma *et al.* [12] who found a concentration ratio of 6. The difference may be the result of different cell lines used showing different functional Pgp expression or variations in the pharmacological Pgp blocking by the inhibitors used (verapamil *vs.* GF120918). In conclusion, the tracers analyzed in our assay showed pronounced differences in the cellular uptake as well as in their potential of being a

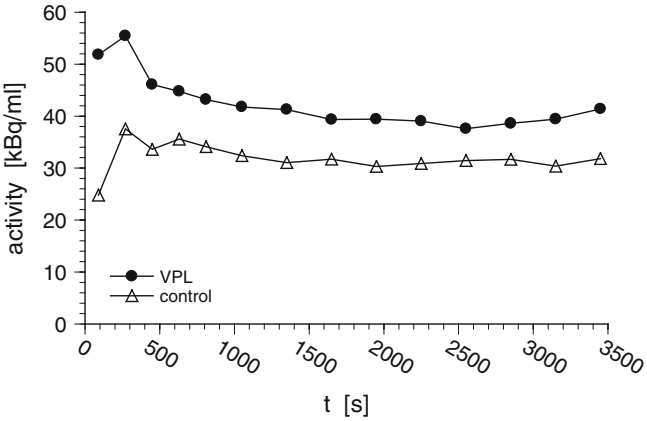

Fig. 11. Time activity curve showing *in vivo* blocking experiment with verapamil ("VPL") directly injected in one tumor of the animal prior to injection of the tracer ^{68}Ga–MFL6.MZ. For control, the contralateral tumor is also presented.

substrate for Pgp. As the compound ^{68}Ga–MFL6.MZ showed the best compromise concerning absolute uptake and inhibition ratio, it was chosen for *in vivo* experiments.

Since Pgp is an active drug transporter depending on ATP as an energy source, the withdrawal of energy may be a mechanism by which Pgp-related chemoresistance might be counteracted [20]. However, since previous studies showed that even a complete glucose deprivation of tumor cells does not affect the functional Pgp activity [21] (presumably due to energy production via other metabolic pathways), it is not expected that glucose depletion affects the cellular distribution of the Pgp tracers.

Biodistribution experiments (Table 2) demonstrated that this ^{68}Ga-labeled complex was mostly accumulated in the liver and the kidney but also in the heart and spleen. Organs which express high levels of Pgp activity (e.g., brain or testis [1]) but also the multidrug-resistant AT1 tumors used in the present study show lower tracer concentrations. These results are in accordance with data for other SPECT (^{99m}Tc-Sestamibi [6]) or PET [12, 13, 22] tracers. Comparing the biodistribution data of ^{68}Ga–MFL6.MZ with those of ^{68}Ga–ENBDMPI [13] revealed that on average the tissue-to-blood ratio of the new tracer was slightly lower, however the variability between the different organs was comparable in its range. The differences between the two tracers may be the result of using different animal models in both studies (rats *vs.* mice) [13]. PET imaging (Figs. 8 and 9) as well as biodistribution measurements [13] reveal that the accumulation in the tumor is in the same magnitude as in the skeletal muscle. For this reason, the imaging contrast between these two tissues is not very high. However, the tracers developed in the present study are not aimed at identifying tumors but at determining the Pgp activity in these tumors. For this reason, a high tumor-to-muscle contrast is not needed. In addition, many of the chemoresistant tumors are not located within the muscle but in the fat tissue (e.g., mammary carcinomas), the lung or bone (e.g., metastases), or the abdominal cavity (e.g., prostate carcinomas). In these tissues, mostly a good contrast between tumor and the surrounding tissue is obtained.

In the *in vivo* experiments with two tracers (^{68}Ga–ENBDMPI and ^{68}Ga–MFL6.MZ), intratumoral concentration was markedly higher than in the testis (reference region in the field of view of the PET images). The intratumoral level of ^{68}Ga–MFL6.MZ was significantly higher (factor 1.74) than for ^{68}Ga–ENBDMPI (Figs. 7 and 8). These results correspond well with the *in vitro* data (Fig. 6) where ^{68}Ga–ENBDMPI showed a much lower intracellular accumulation. To test whether the intratumoral concentration depends on the functional transport activity, Pgp was blocked by verapamil. Since VPL cannot be applied systemically at the necessary concentration, a small amount of VPL was injected directly intratumorally leading to a marked increase in the tracer accumulation as a result of Pgp inhibition (Figs. 9–11). Since the intratumoral ^{68}Ga-activity may depend on the injected dose of or other physiological properties (e.g., systemic blood pressure as the driving force of perfusion), the contralateral tumor served as control. Other groups have used the difference of the intratumoral tracer accumulation in Pgp-expressing and Pgp-negative tumors as an indication of the Pgp specificity of the tracer [7, 13, 23]. One problem of the procedure of the present study may be pressure artifacts by direct intratumoral injection. However, the injected volume was rather small (20 μL), and for comparison, the same amount of solvent was injected contralaterally. For this reason, the increase in tracer concentration after VPL injection is solely by inhibition of Pgp.

The μ-PET studies revealed in the tumors of a volume between 1 and 2 mL that the tracer was heterogeneously distributed (Fig. 10). Since the morphological structure in these tumors does not show differences (homogeneous cell distribution, no necrosis), the differences might be caused by either inhomogeneous Pgp expression or functional heterogeneities of the transporter activity. By immunohistological staining, it was seen that the Pgp expression does not show pronounced differences (data not shown). For this reason, the differences are presumably the result of functional differences which in turn might arise from variations of the local pH. Previous studies using the same tumor model could demonstrate that an extracellular acidosis increases Pgp transport activity markedly [14, 24]. Therefore, regional differences in the tracer distribution can originate from local pH gradients. However, further studies need to elucidate whether the pH indeed affects the PET tracer accumulation due to altered Pgp activity.

In conclusion, the present study describes modified ^{68}Ga-labeled Schiff base ligand-based PET tracers for effectively assessing the functional activity of Pgp *in vivo*. Varying the molecular structure of the complex ligands, tracers with optimal properties can be identified. These tracers shall be used in the future to, for example, optimize the treatment planning by identifying patients with chemoresistant tumors. In parallel, these compounds could also be helpful for tumor biological studies on the impact of metabolic parameters (e.g., pH) on the functional activity of Pgp or for the development of clinically applicable Pgp inhibitors.

Acknowledgments. The study was supported by the European Union (project COST D38 and BM0607) and the Deutsche Krebshilfe (grant 109136).

Conflict of Interest Disclosure. The authors declare that they have no conflict of interest.

References

1. Schinkel AH, Jonker JW (2003) Mammalian drug efflux transporters of the ATP binding cassette (ABC) family: an overview. Adv Drug Deliv Rev 55:3–29
2. Higgins CF (2001) ABC transporters: physiology, structure and mechanism—an overview. Res Microbiol 152:205–210
3. Chang G (2003) Multidrug resistance ABC transporters. FEBS Lett 555:102–105
4. Fojo T, Bates S (2003) Strategies for reversing drug resistance. Oncogene 22:7512–7523
5. Hendrikse NH, Franssen EJ, van der Graaf WT, Vaalburg W, de Vries EG (1999) Visualization of multidrug resistance in vivo. Eur J Nucl Med 26:283–293

6. Liu Z, Stevenson GD, Barrett HH, Kastis GA, Bettan M, Furenlid LR et al (2004) Imaging recognition of multidrug resistance in human breast tumors using ^{99m}Tc-labeled monocationic agents and a high-resolution stationary SPECT system. Nucl Med Biol 31:53–65
7. Kurdziel KA, Kalen JD, Hirsch JI, Wilson JD, Agarwal R, Barrett D et al (2007) Imaging multidrug resistance with 4-[^{18}F]fluoropaclitaxel. Nucl Med Biol 34:823–831
8. Vaalburg W, Hendrikse NH, Elsinga PH, Bart J, Van WA (2005) P-glycoprotein activity and biological response. Toxicol Appl Pharmacol 207:257–260
9. Hsiao P, Sasongko L, Link JM, Mankoff DA, Muzi M, Collier AC et al (2006) Verapamil P-glycoprotein transport across the rat blood-brain barrier: cyclosporine, a concentration inhibition analysis, and comparison with human data. J Pharmacol Exp Ther 317:704–710
10. Zhernosekov KP, Filosofov DV, Baum RP, Aschoff P, Bihl H, Razbash AA et al (2007) Processing of generator-produced ^{68}Ga for medical application. J Nucl Med 48:1741–1748
11. Asti M, De Pietri G, Fraternali A, Grassi E, Sghedoni R, Fioroni F et al (2008) Validation of ^{68}Ge/^{68}Ga generator processing by chemical purification for routine clinical application of ^{68}Ga-DOTATOC. Nucl Med Biol 35:721–724
12. Sharma V, Beatty A, Wey SP, Dahlheimer J, Pica CM, Crankshaw CL et al (2000) Novel gallium(III) complexes transported by MDR1 P-glycoprotein: potential PET imaging agents for probing P-glycoprotein-mediated transport activity *in vivo*. Chem Biol 7:335–343
13. Sharma V, Prior JL, Belinsky MG, Kruh GD, Piwnica-Worms D (2005) Characterization of a ^{67}Ga/^{68}Ga radiopharmaceutical for SPECT and PET of MDR1 P-glycoprotein transport activity in vivo: validation in multidrug-resistant tumors and at the blood–brain barrier. J Nucl Med 46:354–364
14. Thews O, Gassner B, Kelleher DK, Schwerdt G, Gekle M (2006) Impact of extracellular acidity on the activity of p-glycoprotein and the cytotoxicity of chemotherapeutic drugs. Neoplasia 8:143–152
15. Workman P, Twentyman P, Balkwill F, Balmain A, Chaplin DJ, Double JA et al (1998) United Kingdom Co-ordinating Committee on Cancer Research (UKCCCR) Guidelines for the Welfare of Animals in Experimental Neoplasia (2nd edit.). Br J Cancer 77:1–10
16. Kunikane H, Zalupski MM, Ramachandran C, Kuruga MA, Lucas D, Ryan JR et al (1997) Flow cytometric analysis of p-glycoprotein expression and drug efflux in human soft tissue and bone sarcomas. Cytometry 30:197–203
17. Hendrikse NH, de Vries EG, Eriks-Fluks L, van der Graaf WT, Hospers GA, Willemsen AT et al (1999) A new *in vivo* method to study P-glycoprotein transport in tumors and the blood–brain barrier. Cancer Res 59:2411–2416
18. Syvänen S, Blomquist G, Sprycha M, Höglund AU, Roman M, Eriksson O et al (2006) Duration and degree of cyclosporin induced P-glycoprotein inhibition in the rat blood–brain barrier can be studied with PET. Neuroimage 32:1134–1141
19. Wang JH, Scollard DA, Teng S, Reilly RM, Piquette-Miller M (2005) Detection of P-glycoprotein activity in endotoxemic rats by ^{99m}Tc-sestamibi imaging. J Nucl Med 46:1537–1545
20. Xu RH, Pelicano H, Zhou Y, Carew JS, Feng L, Bhalla KN, Keating MJ, Huang P (2005) Inhibition of glycolysis in cancer cells: a novel strategy to overcome drug resistance associated with mitochondrial respiratory defect and hypoxia. Cancer Res 65:613–621
21. Trach P, Afahaene N, Nowak M, Thews O (2008) Impact of environmental parameters on the activity of the p-glycoprotein. Acta Physiol 192(suppl 663):107
22. Bigott HM, Prior JL, Piwnica-Worms DR, Welch MJ (2005) Imaging multidrug resistance P-glycoprotein transport function using microPET with technetium-99 m-sestamibi. Mol Imaging 4:30–39
23. Marian T, Szabo G, Goda K, Nagy H, Szincsak N, Juhasz I et al (2003) In vivo and in vitro multitracer analyses of P-glycoprotein expression-related multidrug resistance. Eur J Nucl Med Mol Imaging 30:1147–1154
24. Sauvant C, Nowak M, Wirth C, Schneider B, Riemann A, Gekle M et al (2008) Acidosis induces multi-drug resistance in rat prostate cancer cells (AT1) in vitro and in vivo by increasing the activity of the p-glycoprotein via activation of p38. Int J Cancer 123:2532–2542